Differential Displacement and Strain Analysis of Transmission Line Cables

Adriana Lima Rolim
alrolim@gmail.com
Federal University of Pará
Civil Engineering College
66075-110, Belém, Pará, Brazil

Jouberson L. da R. Moreira
jouberson@hotmail.coml
Federal University of Pará
Mechanical Engineering College
66075-110, Belém, Pará, Brazil

Luis A. C. M. Veloso
lveloso@ufpa.br
Federal University of Pará
Civil Engineering College
66075-110, Belém, Pará, Brazil

Remo Magalhães de Souza
remo@ufpa.br
Federal University of Pará
Civil Engineering College
66075-110, Belém, Pará, Brazil

José Alexander Araújo
alex07@unb.br
University of Brasília
Department of Mechanical Engineering
70910-900, Brasília, Distrito Federal, Brazil

This paper presents a strain analysis in transmission line cables caused by mechanical vibrations induced mainly by the wind action that can cause the fatigue rupture of the cable. The tests were performed on a test bench that consists of two spans of 9 and 12 meters respectively, and it was built using elements of transmission lines (suspension clamps, insulators, anchoring towers, etc). The vibrations were generated by an electrodynamics shaker. Strains were measured by means of micro-electric strain gauges set in 04 wires of the cross section of the cable at the vicinity of the suspension clamp, which presents severe levels of dynamic stresses. The cable bending amplitude was measured with two laser transducers. The bending amplitude was converted in strain with the Poffenberger-Swart equation. The comparison between the measured strain and the predicted theatrically showed RMS errors of 31% and 48% for axial load levels of 20%UTS and 30%UTS, respectively.
Keywords: *Aeolian Vibration, Transmission Lines, Fatigue, Cables.*

Introduction

Overhead transmission line cables in their real configuration, installed on top of the towers, are exposed to Aeolian vibrations. These vibrations are a high frequency motion that can occur when a smooth, steady crosswind blows on aerial cables. This laminar wind creates vortices, which are detached at regular intervals on the leeward side, alternating from top and bottom of the cable. The detachments create vertical forces causing the cable to vibrate standing waves generally in high harmonic modes.

The cyclic nature of these vibrations can produce fatigue that is, according to the EPRI (1979), the most usual kind of damage produced by the Aeolian vibrations in the transmission line cables and they can also produce damage in other components of the line such as dampers, armour rods and tower members. This kind of damage is more usual in regions where the mechanical behaviour of the cable is restrained such as regions near from suspension clamps, spacer clamps and dampers, Rawlins (1997).

Fatigue failure is frequently unexpected and unwarned, with difficult identification and when it happens in transmission line cables, the electric energy supply is interrupted causing blackouts in regions and cities.

From the point of view of mechanical behavior, the transmission line cables exhibits a complex behavior because its transversal section is constituted of layers, sometimes of different materials, formed of strands disposed helicoidally. The bending stiffness of the conductor depends on the conductor deformation during the bending process, i. e. it varies not only spatially along the conductor but also during the bending cycle (loading-unloading). This variation influences the conductor displacement and the conductor curvature, which in turn affects the conductor bending stiffness, Papailiou (1997).

Therefore, in a same cable the inertia moment of the section can be variable along its axis as a function of the friction level among the strands. This fact can be observed through the abrasion marks in tested cables that are more evident near the clamp and less evident far from it, Poffenberger and Swart (1965).

Since forties of last century, many researchers have been made to evaluate the mechanical vibration stresses in transmission line cables for the fatigue analyses. However, the Poffenberger-Swart equation that treats the problem with many simplifications is still recommended for the EPRI to evaluate the cable stress due to mechanical vibrations. Many of the tests used to validate this equation have been conducted comparing the mechanical stress measured with strain gages with the data obtained with the Poffenberger-Swart equation using tests apparatus with rigid cable clamps that normally do not represent the real conditions of transmission lines.

In this work, a transmission line cable was tested in laboratory for various levels of frequency and bending amplitude using a test setup that tried to simulate the typical Brazilian configuration of a transmission line with the use of an articulated suspension clamp. Mechanical strains measured with micro strain gages installed on the cable near from the suspension clamp were compared with the ones obtained by Poffenberger-Swart equation. Also, the experimental loop lengths values measured along the tests were compared with the theoretical values.

Paper submitted in ??/?? and accepted in ??/????. Technical Editor ???

Nomenclature

a = *horizontal distance of L1 laser transducer to the clamps´s centre of rotation, m*
A = *standarized distance of 89 mm from the last point of contact between the cable and the clamp*
b = *constant of integration*
d = *wire diameter, m*
E = *Young modulus, N/m²*
EI = *bending stifness, N.m²*
f = *frequency, Hz*
I = *area moment of inertia, m⁴*
j = *stiffness parameter, m*
k = *bending curvature,1/ m*
L = *loop lenght, m*
m = *mass per unit length, kg/m*
M = *bending moment, N.m*
M_0 = *couple, N.m*
n = *sample size*
n_L = *number of loops*
S = *span lenght , m*
T = *traction load, N*
V_t = *travel wave velocity, m/s*
V_T = *accurate trvelling wave velocity, m/s*
x = *horizontal axis*
y = *deflectin, m*
y_a = *bending amplitude (peak to peak), m*
y´´ = *second derivatives of y, 1/ m*
w = *transverse load, N/m*

Greek Symbols

$\Delta\beta$ = rotation angle, *rad*
Δ_{L1} = displacement measured with L1 laser transducer
Δ_{L2} = displacement measured with L2 laser transducer
ε = strain amplitude (zero to peak), m/m
λ = dimensionless parameter of Poffenberger-Swart equation
θ = rotation angle, *rad*
ϕ = dimensionless parameter of Poffenberger-Swart equation

Subscripts

a relative to distance
L relative to loop
t relative to the travel wave velocity
T relative to the accurate travelling wave velocity
0 relative to the maximum amplitude (w) or to a couple (M)
max relative to maximum
min relative to minimum
slip relative to maximum friction stress which act on each wire
stick relative to the situation when all wires stick together as a solid body

Theoretical Aspects of the Measurement

Measurement Principle

The measurement of Aeolian vibration of overhead conductors was standardised in 1965 by IEEE Committee, which authorized the formation of a group in 1961 to investigate the problem. It was the Task Force on Standardization of Conductor Vibration Measurements. Their purpose was to evaluate various means of assessing conductor vibration and to recommend a standard method, IEEE (1966).

According to IEEE (1966), several practical parameters have been employed in the past. One parameter was the angle of bending imposed on the conductor at the clamp, as inferred from measurement of free loop amplitude and loop length. This inference could be accurate only when the clamp was stationary and free of rocking, conditions that could not be assumed for the articulated suspension clamps of transmission lines.

The bending amplitude was adopted since 1965 rather than any other displacement to measure the conductor vibration. It was introduced in 1941, Tebo (1941), and proposed for general use in 1963, Edwards and Boyd (1963). It was defined as the peak-to-peak dynamic conductor displacement with respect to the suspension clamp at 89 mm from their last point of contact.

In most cases, the critical points where there are high stress levels are located at the last point of contact (LPC) between the conductor and the bed of the suspension clamp due to the fact that the fretting occurs usually at locations where the transverse mobility of the conductors is dynamically restrained to the movement induced by the Aeolian vibrations, mainly vertical displacements.

Therefore, in the experimental tests with ACSR conductors to measure maximum strains and stresses, the strain gages were mounted on wires at cross sections located at LPC, as can be seen in Fadel et. al (2011) and Lévesque et. al (2010).

Conductor Models

The Poffenberger-Swart equation represents a mathematical solution defining the relationship between dynamic flexural strain and differential displacement, or bending amplitude. This formulation was described in details in Poffenberger and Swart (1965) and Grodreau at. al (2010a). They treat the cable as a straight beam under a sinusoidal distributed transverse load with an axial load applied on it. The deformed configuration of the cable is also considered as sinusoidal, Fig 1.

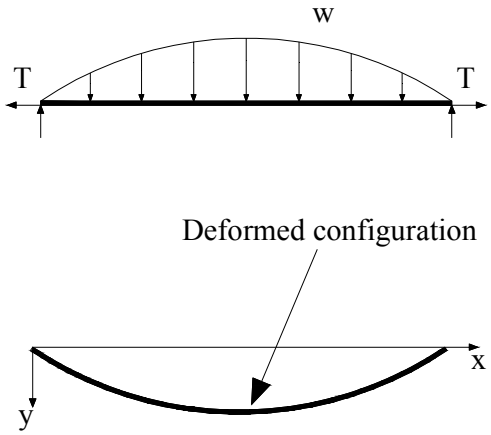

Figure 1. Cable configuration under load

On the development of the deflection equation, Poffenberger and Swart considered for first a simple supported beam under a sinusoidal distributed transverse load and tension, Fig. 2-a. Next, they considered a member acted upon by a couple at one end and the same axial tensile loading, Fig 2-b.

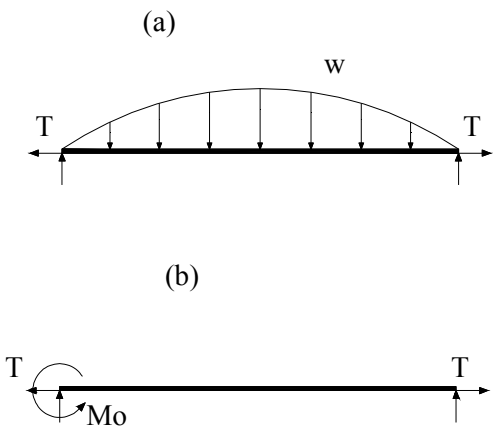

Figure 2. Superposition problem. (a) Beam under transverse load and tension. (b) Beam under couple, where the couple represents the action of the clamp

Then, these two equations were combined, a superposition of the two previously cases to provide a general solution for a tensile member with a couple at one and a sinusoidal distributed transverse loading.

The bending moment at any point of the conductor can be determined by Eqs. (1) and (2) for the first and second cases, respectively.

$$M(x) = \frac{w_0}{b^2} senbx - Ty \tag{1}$$

$$M(x) = -M_0\left(1 - \frac{x}{L}\right) - Ty \tag{2}$$

where: T – traction load; L – loop length.

The bending curvature of the conductor is assumed to be given by the usual solid beam equation, Eq.(3).

$$y'' = -\frac{M(x)}{EI} \tag{3}$$

It is also assumed that each strand of the conductor bends independently from another, i. e. the strands are free to move relatively to each other. This individual strand approach implies that bending stiffness of the conductor takes its minimal possible value, given by the sum of the bending stiffness of all conductor strands, Papailiou (1997). However, this assumption may not fit with experimental data in some cases, Lévesque et. al (2010)

Substituting Eq. (1) and Eq. (2) into Eq. (3) and solving the differential equations, the deflection equation can be calculated with Eq. (4) and Eq. (5) for the first and second cases, respectively.

$$y = \frac{w_0 L^2 \lambda_2 sen(\pi x/L)}{T\pi^2(\pi^2 + \lambda^2)} \tag{4}$$

$$y = -\frac{M_0}{T}(senh\phi \coth\lambda - \cosh\phi + 1 - \frac{x}{L}) \tag{5}$$

where: $j^2 = EI/T$; $\quad \phi = x/j$; $\quad \lambda = L/j$

The general solution is the sum of Eq. (4) and Eq. (5) and considering geometric and trigonometric approximations resulting in the Eq. (6) that calculates the deformed configuration of the conductor. This general equation can be applied to a fixed-hinged member or any member with one end partially fixed.

$$y_a = \frac{M_0}{T}\left(e^{-A/j} - 1 + \frac{A}{j}\right) \tag{6}$$

where: y_a – bending amplitude and A– 89 mm from the last point of contact between the cable and the clamp.

Taking Eq. (6), assuming a linear behaviour of the conductor and a linear distribution of the stresses along the strands, the strain at 89 mm from the last point of contact between the cable and the clamp can be estimated by Poffenberger-Swart formula, as follows:

$$\varepsilon = \frac{y_a d}{2j(e^{-\frac{A}{j}} - 1 + \frac{A}{j})} \tag{7}$$

where: ε – strain amplitude (zero to peak); y_a – bending amplitude (peak to peak); j – stiffness parameter, root square of the relation between EI and the axial load T; d – wire diameter; A– 89mm from the last point of contact between the cable and the clamp.

A drawback of this model is that it does not consider properly the inner conductor structure (cross section configuration) and in particular the interlayer friction.

Papailiou (1997) presents a model for conductors under simultaneous tensile and bending loads. The proposed model takes into account the interlayer friction and the interlayer slip in the conductor during bending and leads to a variable bending stiffness, which varies not only along the conductor but also during the bending cycle. The bending stiffness of the conductor depends on the slip, Fig 3.

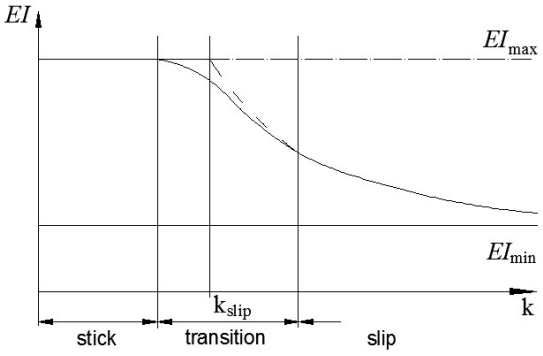

Figure 3. Conductor bending stiffness EI as a function of the curvature k, Papailiou (1997)

In cases where all wires stick together as a solid body, the bending stiffness of the conductor is:

$$EI_{\max} = EI_{\min} + EI_{stick} = const. \quad (8)$$

where: EI_{min} – minimum bending stiffness that considers only the bending resistance of the individual wires about their own neutral axis; EI_{stick} –additional term to the bending stiffness when all wires stick together as a solid body.

And in case of slip, the bending stiffness of the conductor is:

$$EI = EI_{\min} + EI_{slip} = function(curvature, axial\ load) \quad (9)$$

where: EI_{slip} – bending stiffness that takes into account the maximum friction stress which act on each wire.

Because of the presence of the interlayer friction, this conductor model is non-linear needing to be solved with a numerical procedure such as the Finite Element Method.

Goudreau et al. (2010b) showed that by using a simplified bending model of the conductor related to the support geometric characteristics, such as the radius of curvature of the clamp, it is possible to obtain better correlations with experimental data. This conductor model is developed observing the static equilibrium of the bending moment of the conductor subjected to the traction load T near the clamp and the tangent angle at the point of last point of contact (LPC) between the conductor and the bed of the suspension clamp, Fig 4-a.

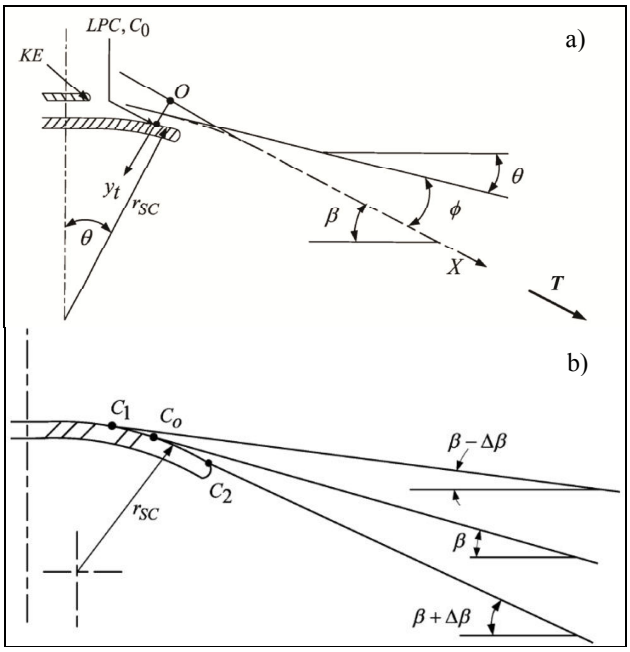

Figure 4. Clamps parameters, Goudreal et al. (2010b). (a) Generic suspension clamp (conductor not shown). (b) Contact circular arc of the conductor under vibration

Goudreau et al. (2010b) concluded that the conductor model is greatly influenced by the length of the contact circular arc xC2-C1 governed by Δβ which is the rotation of the Y-X axis system following the contact movement of the conductor on the suspension clamp bed, Fig-4b.

Because the new conductor model formulations are too complicated for practical purposes, Poffenberger-Swart equation is still used as fatigue indicators in the S-N diagrams.

Instrumentation and Test Procedure

Tests were performed with a Grosbeak 636 conductor. This cable is formed by two external aluminium layers with a total of 26 wires with 4 millimetres diameter and a steel core with one layer of 6 wires and a central wire, both with 3.1 millimetres diameter, Fig. 5.

The aim of these tests was to measure the conductor bending amplitudes, which were converted in strains by using Eq. (7). These values were then compared with the strains measured directly by means of four micro-strain gages fixed at stands near the clamp, set according to Fig. 6.

The strain gage measurements are considered as the "real" strains at the conductor because they were measured directly without additional hypotheses. Therefore, they have been used to validate new conductor models in several researches such as Lévesque et. al (2010) and Grodreau at. al (2010b), nevertheless that small deviations may occur with respect to the strain gage distance to the LPC.

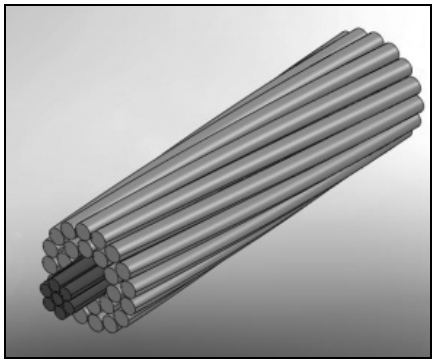

Figure 5. Schematic of the tested cable

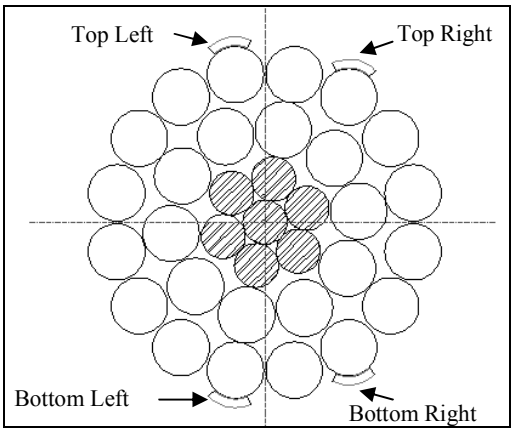

Figure 6. Scheme of the arrangement of the electrical strain gages on the cable

In all tests, the measured strains values acquired were quite similar. In some tests, the measured strains at points more distant from cable axis exhibit the grater values, but in other tests it could not be noticed. Therefore, it was found a more appropriate method to perform the average of the strains. The bending amplitude was

measured 89 mm away from the clamp mouth with two lasers transducers, Fig. 7.

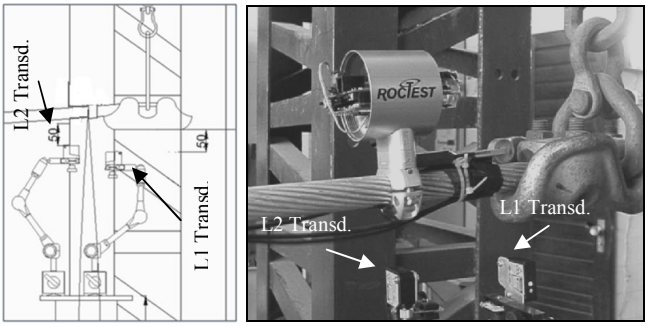

Figure 7. Arrangement of the laser transducers

The clamp rotations provoke rigid body motions of the cable that do not induce bending stresses in the cable. Then, to evaluate the bending amplitude, it was necessary to discount the amount of rigid body displacement, Fig. 8 to Fig. 11.

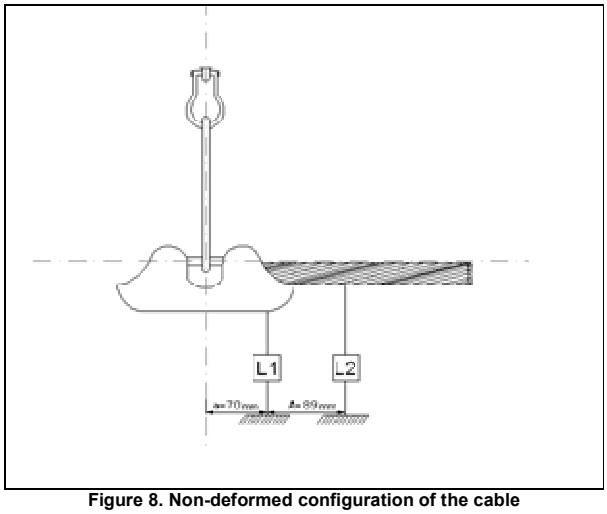

Figure 8. Non-deformed configuration of the cable

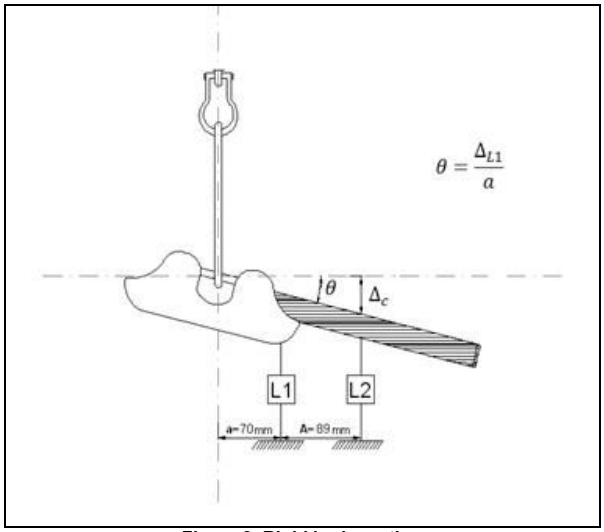

Figure 9. Rigid body motion

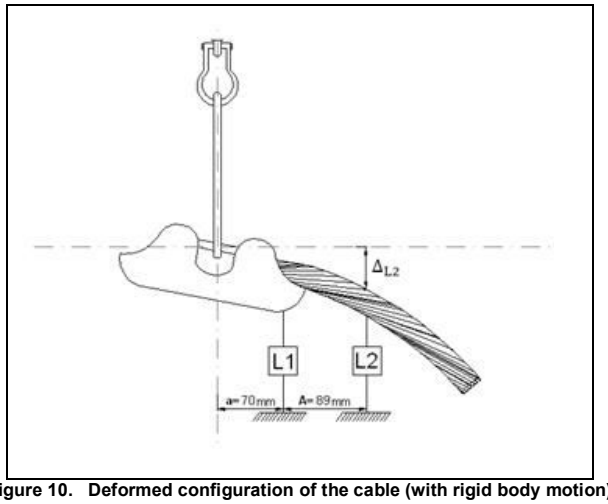

Figure 10. Deformed configuration of the cable (with rigid body motion)

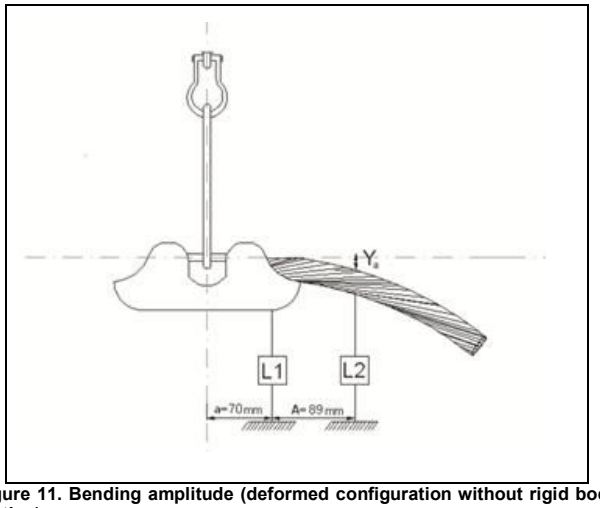

Figure 11. Bending amplitude (deformed configuration without rigid body motion)

According to Fig. 8 to Fig. 11, the laser transducers L1 and L2 measure the displacements of clamp mouth and the cable displacement 89 mm away from the last point of contact between the cable and the clamp, respectively. The bending amplitude is evaluated with the displacements of the two laser transducers with the Eq.(10).

$$y_a = \Delta_{L2} - \frac{\Delta_{L1}}{a}(a + A) \tag{10}$$

where: $\Delta L1$– displacement measured with L1 laser transducer; $\Delta L2$– displacement measured with L2 laser transducer; a – is the horizontal distance of the L1 laser transducer to the clamp´s centre of rotation; A – is 89mm from the last point of contact between the cable and the clamp.

The tests were conducted with two different levels of mean axial load: 22060 N and 33100 N. These values correspond respectively to 20% and 30% of the UTS, Ultimate Tension Strength, according to the NBR-7270 (1988). The 30% UTS load level is higher than the usual pre-loads found in real transmission lines but it was tested to investigate the cable behaviour under such conditions.

An electromagnetic shaker and a sinusoidal signal generator were used to induce mechanical vibrations on the cable, Fig. 12.

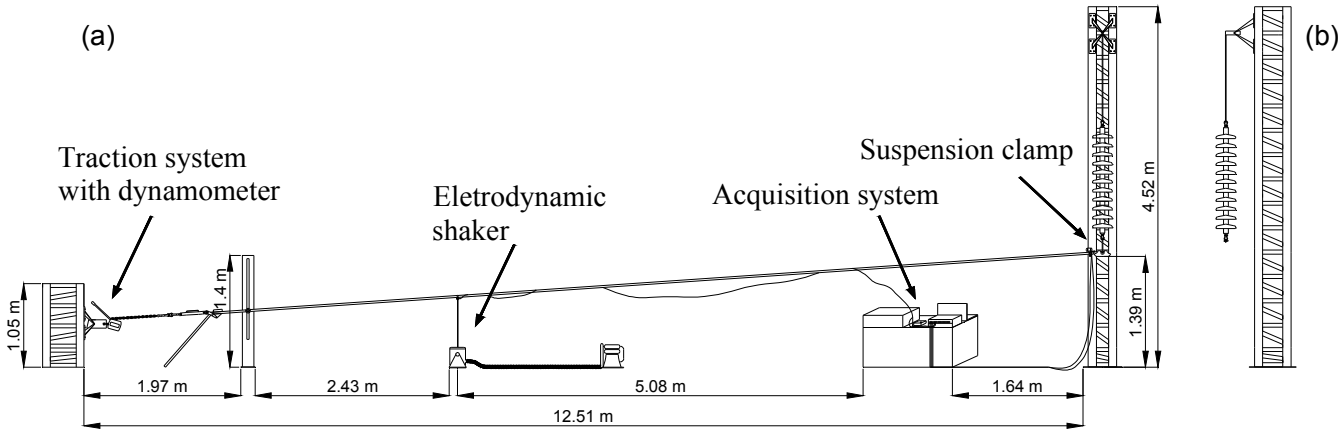

Fig 12a. Experimental test setup

Fig 12b. Lateral view

Initially, it was planned to consider five different amplitudes ΔL2 (0.05, 0.1, 0.2, 0.3 and 0.4 mm) and excitation frequencies (10, 20, 30, 40 and 50 Hz) for each axial load level, resulting in 25 tests per traction level, hence totalizing 50 different tests. However, at some of these tests the shaker could not work adequately. An overall of 20 tests were performed for the 20% UTS and 19 for the 30% UTS totalizing 39 different tests.

Results

Experimental Strain-Displacement Data

Figure 13 and Fig. 14 show the measured strains by means of the strain gages and the strains estimated with the Poffenberger-Swart equation represented by the straight line, as a function of the bending amplitude for the 20% and 30% UTS, respectively.

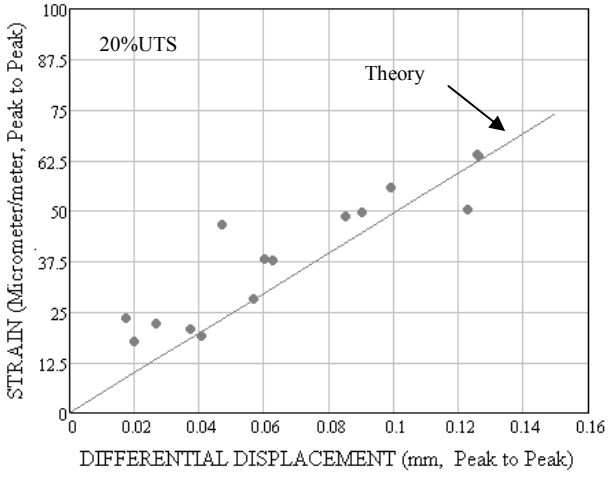

Figure 13. Experimental strain-displacement data for Grosbeak 636 conductor (20% UTS)

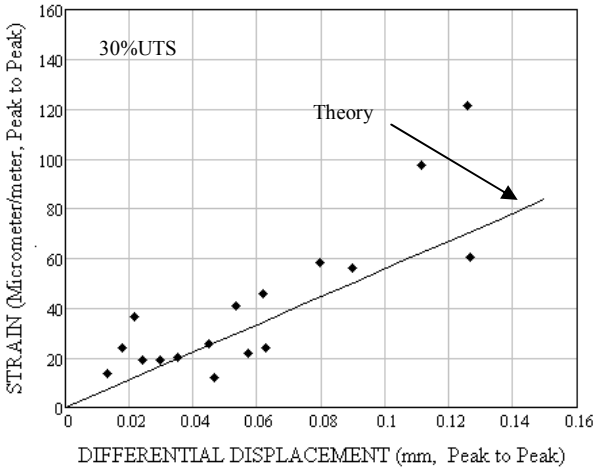

Figure 14. Experimental strain-displacement data for Grosbeak 636 conductor (30% UTS)

The experimental data depicted in Fig. 13 and Fig. 14 show that it is reasonable to assume that there is a linear relation of the bending amplitude and the corresponding strain for the two axial load levels considered. Some points, mainly for the 30% UTS level, are far from the straight line, which yields the predicted strain. It is likely that, in these situations, either occurred some level of slip among the aluminium wires, cable resonance or other type of nonlinearities that were not considered in the formulation by Poffenberger-Swart.

The experimental data contained in Fig. 13 and Fig. 14 are displayed in Fig. 15 to Fig. 19 according to the excitation frequency of the vibrations used in the tests.

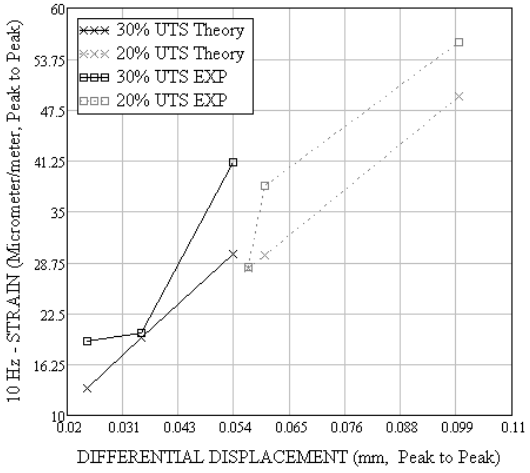

Figure 15. Experimental strain-displacement data for Grosbeak 636 conductor for the excitation frequency of 10 Hz

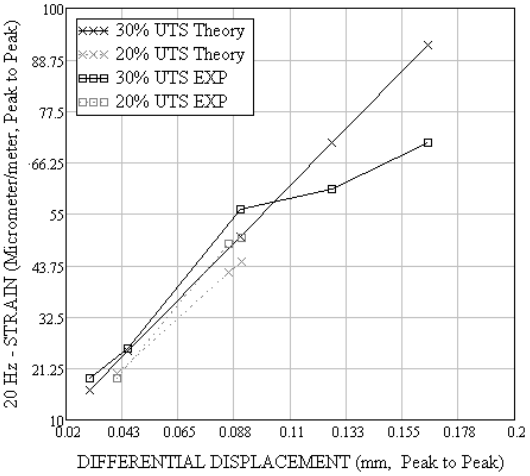

Figure 16. Experimental strain-displacement data for Grosbeak 636 conductor for the excitation frequency of 20 Hz

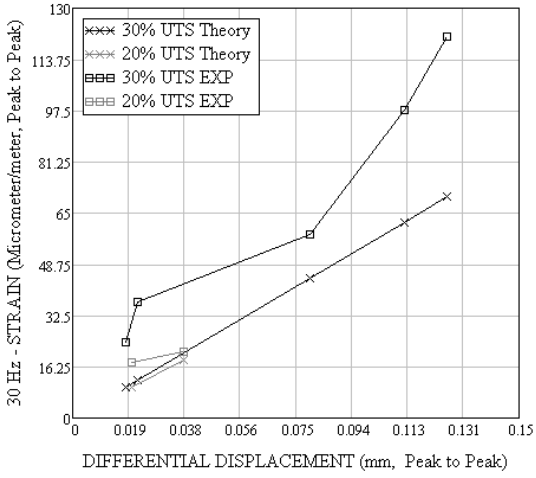

Figure 17. Experimental strain-displacement data for Grosbeak 636 conductor for the excitation frequency of 30 Hz

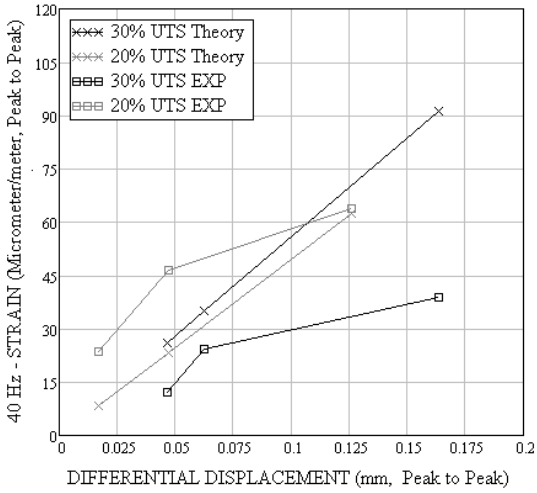

Figure 18. Experimental strain-displacement data for Grosbeak 636 conductor for the excitation frequency of 40 Hz

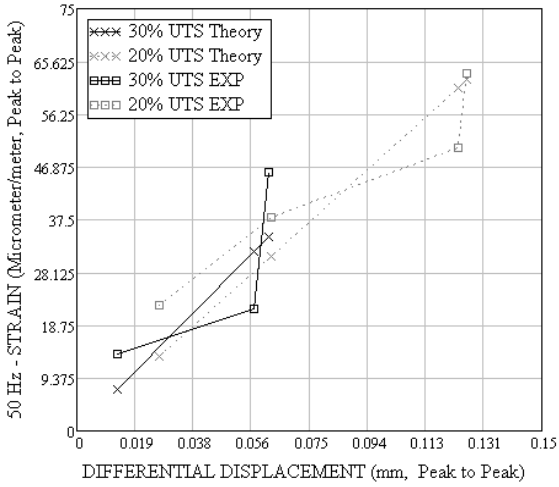

Figure 19. Experimental strain-displacement data for Grosbeak 636 conductor for the excitation frequency 50 Hz

After evaluating the data contained in Fig. 15 and Fig. 19, it is possible to conclude that at excitation frequencies of 20 Hz there is a better agreement among measured strains and the theoretical values. On the other hand, large differences between measured and theoretical data were obtained for both axial load levels at an excitation frequency of 40 Hz. Tables 1 and 2 show an error comparison of these data using Eqs. (11) and (12).

$$E(\%) = \frac{\varepsilon_{th} - \varepsilon_{sg}}{\varepsilon_{sg}} \times 100 \tag{11}$$

$$RMSE(\%) = \sqrt{\frac{\left(\sum_{1}^{n} \frac{\varepsilon_{th} - \varepsilon_{sg}}{\varepsilon_{sg}}\right)^2}{n}} \times 100 \tag{12}$$

where: $E(\%)$– "standard" error; $RMSE(\%)$ – root mean square error; ε_{th} – theoretical strains; ε_{sg} – measured strains; n – sample size.

Tables 1 and 2 report the total RMSE errors calculated with Eq. (12) considering all tests at the same traction load level. The total RMSE errors are 31% and 48% when using the Poffenberger-Swart equation to predict the cable strain near the cable clamp for the traction levels of 20% and 30% UTS, respectively. The largest differences were observed for the tests under 30% UTS level and at a 40 Hz frequency, where the strains evaluated theoretically are approximately 100% larger than the measured ones.

Table 1 – Comparison between measured and theoretical strains, 20% UTS

Freq. (Hz)	Diff. Displ. (mm)	Error (%)	RMSE (%)	Total RMSE (%)
10	0.057	-0.3	19.9	31.4
	0.060	-22.3		
	0.099	-11.9		
20	0.041	5.7	10.2	
	0.085	-13.3		
	0.090	-10.1		
	0.041	5.7		
30	0.020	-44.4	39.7	
	0.037	-11.8		
40	0.017	-63.8	67.1	
	0.047	-50.0		
	0.126	-2.5		
50	0.027	-40.6	19.8	
	0.063	-17.9		
	0.123	20.8		
	0.126	-1.9		

Table 2 – Comparison between measured and theoretical strains, 30% UTS

Freq, (Hz)	Diff. Displ. (mm)	Error (%)	RMSE (%)	Total RMSE (%)
10	0.024	-29.9	25.9	48.3
	0.035	-2.8		
	0.054	-27.3		
20	0.030	-13.2	19.2	
	0.045	-2.1		
	0.090	-10.5		
	0.127	16.8		
	0.165	30.0		
30	0.036	-59.1	53.4	
	0.044	-67.0		
	0.16	-23.9		
	0.222	-36.3		
	0.252	-42.1		
40	0.047	112.6	106.4	
	0.063	44.4		
	0.163	134.6		
50	0.013	-47.0	50.1	
	0.057	46.9		
	0.062	-25.0		

Loop Lengths Comparison

During the tests some measurements of the cable loop length were obtained for each excitation frequency level, for both traction levels, 20% and 30% UTS. The experimental values were then compared with theoretical results obtained by the relation between the span length and the number of loops, Eq. (13).

$$L = \frac{S}{n_L} \tag{13}$$

where: L – loop length (half of the wave length); S – span length; n_L – number of loops.

The number of loops was obtained by means of the Eq. (13.1).

$$n_l = \frac{2Sf}{V_T} \tag{13.1}$$

where: S – span length; f– frequency; V_T – accurate travelling wave velocity.

The travel wave velocity was calculated using Eq. (13.2).

$$V_t = \sqrt{\frac{T}{m}} \tag{13.2}$$

where: T– traction load; m– mass per unit length of the cable.

In the sequence, an equation proposed by EPRI (1979) that incorporates the stiffness parameter to the wave velocity was used in order to obtain accurate results.

$$V_T = V_t\left[1+\left(\frac{2\pi^2 f^2 mEI_{\max}}{T^2}\right)\right] \tag{13.3}$$

where: f – frequency; Vt – travelling wave velocity; V_T – accurate travelling wave velocity; m – mass per unit length of the cable; EI_{max} – maximum bending stiffness.

The theoretical values of loop length are compared with the measured loop lengths and these values are presented in Table 3 and Table 4 for the traction levels of 20% UTS and 30% UTS, respectively.

Table 3. Loop Length (m) - 20% UTS

Freq (Hz)	Exp.	Theory	Error (%)	RMSE (%)
10	6.40	6.56	2.5	7.7
20	2.80	3.27	16.8	
30	2.10	2.18	3.8	
40	1.62	1.63	0.6	
50	1.20	1.31	9.2	

Table 4. Loop Length (m) –30% UTS

Freq (Hz)	Exp.	Theory	Error (%)	RMSE (%)
10	8.55	8.03	-6.2	7.8
20	3.45	4.01	16.2	
30	2.64	2.68	1.5	
40	2.09	2.01	-3.8	
50	1.70	1.60	-5.9	

Data reported in Tables 3 and 4 show a good agreement between the measured and the calculated loop length and similar RSME for 20% and 30% UTS traction levels.

Conclusions

The tests conducted tried to simulate, as real as possible, the typical Brazilian configuration of a transmission line using an articulated suspension clamp. Although small deviations may occur with respect to the strain gage distance to the LPC, the strain gage measurements are considered as the "real" strains at the conductor because they were measured directly without additional hypotheses. Therefore, the measured strains were used to validate the theoretical strains. The experimental data exhibit tendencies of linear relation of the bending amplitude and the corresponding strain for the two tractions levels. Some points, mainly for the 30% UTS level, are far from the straight line that corresponds to the predicted strain. It is likely that in these situations occurred phenomena such as partial interaction among wires, cable resonance or nonlinearities that are not considered in the formulation of Poffenberger-Swart equation. The total RMS errors are 31% and 48% when using the Poffenberger-Swart equation to predict the cable strain near the cable clamp for 20% and 30% UTS levels, respectively. It was found a good agreement between measured and the theoretical loop lengths.

Acknowledgements

The authors would like to thank CNPq – "Conselho Nacional de Desenvolvimento Científico e Tecnológico", of the Brazilian Ministry for Science and Technology and ELETRONORTE – "Centrais Elétricas do Norte do Brasil" for the financial support provided.

References

Cigré, 1979, "Recommendations for the Evaluation of the Lifetime of Transmission Line Conductors", Electra n. 63: WG 04 SC 22 – 02.

Edwards, A. T, Boyd, J. M., 1963, "Ontario Hydro Live-line Vibration Recorder for Transmission Conductors", IEEE Trans. on Power Apparatus and Systems, vol. 82, pp 269-270.

EPRI, 1979, "Wind Induced Conductor Motion, Electrical Power Research Institute", Transmission Line Reference Book, Palo Alto, CA, USA.

IEEE Committee Report, 1966, "Standardization of Conductor Vibration Measurements", IEEE PAS-85, vol. 85, n. 1, 10+22 pp.

Fadel, A.A., Rosa, D., Murça, J.L.A., Ferreira, J. L.A., Araújo, J. A, 2011, "Effect of high mean tensile stress on the fretting fatigue life of an Ibis steel reinforced aluminium conductor". Int. J. Fatigue, doi:10.1016/j.ijfatigue.2011.03.007.

Goudreau, S., Lévesque, F., Cardou, A., Cloutier, L., 2010a, "Strain measurements on ACSR conductors during fatigue tests II – stress fatigue indicators". IEEE Transaction on Power Delivery, Vol. 25, No. 4, pp. 2997-3006.

Goudreau, S., Lévesque, F., Cardou, A., Cloutier, L., 2010b, Strain measurements on ACSR conductors during fatigue tests III – strain related to support geometry". IEEE Transaction on Power Delivery, Vol. 25, No. 4, pp. 3007-3016.

Hardy, C., Brunelle, J., 1991, "Principles of Measurement and Analysis with the New PAVICA Conductor Vibration Recorder", Canadian Electrical Association Centennial Conference, Toronto.

Kraus, M., Hagedorn, P., 1991, "Aeolian Vibrations: Wind Energy Input Evaluated from Measurements on an Energized Transmission Line", IEEE Transactions on Power Delivery, Vol. 6, No. 3.

Lévesque, F., Goudreau, S., Cardou, A., Cloutier, L., 2010, "Strain Measurements on ACSR conductors during fatigue tests I – experimental method and data". IEEE Transaction on Power Delivery, Vol. 25, No. 4, pp. 2825-2834.

NBR-7270, 1988, "Aluminum Cables, Stell-Reinforced for Overhead Lines". Brazilian Code – ABNT, Rio de Janeiro, Brasil.

Papailiou, K.O., 1997 "On the bending stiffness of transmission line conductors". IEEE Transaction on Power Delivery, Vol. 12, No. 4, pp. 1576-1588.

Poffenberger, J. C., Swart R. L., 1965, "Differential Displacement and Dynamic Conductor Strain", IEEE Trans, Paper, Vol. PAS – 84, pp. 281 – 289.

Rawlins, C.B, 1997, "Transactions on Power Delivery, Some Effects of Mill Practice on the Stress Behavior of ACSR", IEEE.

Rolim, A. L., 2009, "Contribution for the Study of Mechanical Stresses due to Aeolian Vibrations in Transmission Line Cables", (in Portuguese), MSc Dissertation, Civil Engineering College, Federal University of Pará, Pará, Brazil.

Tebo, G. B., 1941, "Measurement and Control of Conductor Vibration", Trans. AIEE, vol.60, pp 1188-1193.